The emergence of resonating valence bond physics in spin–orbital models

2007 J. Phys.: Condens. Matter 19 145201

(http://iopscience.iop.org/0953-8984/19/14/145201)

IOP PUBLISHING JOURNAL OF PHYSICS: CONDENSED MATTER

J. Phys.: Condens. Matter **19** (2007) 145201 (9pp) doi:10.1088/0953-8984/19/14/145201

The emergence of resonating valence bond physics in spin–orbital models

F Mila[1], F Vernay[2], A Ralko[1], F Becca[3], P Fazekas[4] and K Penc[4]

[1] Institute of Theoretical Physics, Ecole Polytechnique Fédérale de Lausanne, CH-1015 Lausanne, Switzerland
[2] Department of Physics, University of Waterloo, Waterloo, ON, N2L3G1, Canada
[3] INFM-Democritos, National Simulation Center and International School for Advanced Studies (SISSA), I-34014 Trieste, Italy
[4] Research Institute for Solid State Physics and Optics, H-1525 Budapest, POB 49, Hungary

E-mail: frederic.mila@epfl.ch

Received 11 September 2006
Published 23 March 2007
Online at stacks.iop.org/JPhysCM/19/145201

Abstract

We discuss how orbital degeneracy, which is usually removed by a cooperative Jahn–Teller distortion, could under appropriate circumstances lead rather to a resonating valence bond spin–orbital liquid. The key points are: (i) the tendency to form spin–orbital dimers, a tendency already identified in several cases; (ii) mapping onto quantum dimer models, which have been shown to possess resonating valence bond phases on the triangular lattice. How this programme can be implemented is explained in some detail starting from a microscopic model of $LiNiO_2$.

(Some figures in this article are in colour only in the electronic version)

1. Introduction

It is very useful to classify quantum magnets according to the symmetry (if any) that is broken in the ground state. When $SU(2)$ symmetry is broken, the system usually sustains some kind of long-range magnetic order, although some more exotic examples involving quadrupolar order have recently been discussed [1, 2]. When $SU(2)$ symmetry is not broken, a translation symmetry may or may not be broken depending on the lattice topology. The standard case in which no lattice symmetry is broken is that of systems in which it is possible to build a singlet inside the unit cell, as for instance in a ladder [3]. If, however, this is not possible, as in all systems with half-integer spins and an odd number of sites per unit cell, the simplest way to keep $SU(2)$ symmetry is to break the translation symmetry so that the new unit cell contains an even number of sites per unit cell. A typical example is the $S = 1/2$ $J_1 - J_2$ chain, which was explicitly shown by Majumdar and Ghosh [4] quite some time ago to have a two-fold degenerate dimerized ground state when $J_2 = J_1/2$.

Another possibility to keep $SU(2)$ symmetry without breaking any lattice symmetry was put forward by Anderson [5] in 1973. Concentrating on $S = 1/2$ magnets, he suggested that under appropriate circumstances the ground state might be a linear combination of valence bond (VB) states, i.e. states in which sites are paired to form singlets. Clearly each individual state breaks at least some of the translational symmetries of the underlying lattice, but the translational symmetry is restored by the superposition of such valence bond states. Such a wavefunction is known as a resonating valence bond (RVB) state.

To identify such a ground state in realistic models of quantum antiferromagnets turned out to be much more difficult than anticipated. The prediction of Fazekas and Anderson [6] that this might be the case for the $S = 1/2$ Heisenberg model on the triangular lattice, based on estimates of the energy of ordered and valence bond states including perturbation corrections, is not supported by recent numerical investigations, which all point to three-sublattice antiferromagnetic order [7].

The most serious candidate still around is the $S = 1/2$ Heisenberg antiferromagnet on the kagome lattice. No evidence of magnetic long-range order has been found so far, and the proliferation of low-lying singlets observed in exact diagonalizations of finite clusters [8] can be fairly well described in the short-range RVB subspace of valence bond states involving only nearest neighbours [9]. However, several treatments based on some effective Hamiltonian have reached the conclusion that the ground state supports some kind of valence bond order [10–12], and hence breaks translational symmetry. Unfortunately, the resulting unit cell is so large, and the singlet–singlet gap accordingly so small, that this prediction cannot be cross-checked by the only unbiased numerical approach available so far, namely exact diagonalization, and the issue is likely to remain open for quite some time.

In fact, it has only been possible so far to unambiguously identify an RVB ground state in a very minimal description of fluctuations in the RVB subspace that goes under the name of the quantum dimer model (QDM) [13]. In this approach, valence bond configurations are assumed to build an orthogonal basis of the Hilbert space, and the effective Hamiltonian contains kinetic terms that shift dimers around loops and potential terms that favour or penalize specific local configurations of dimers. For the triangular lattice, the simplest model is defined by the Hamiltonian

$$H = v \sum \left(|\,\rangle\langle\,| + |\,\rangle\langle\,| \right) - t \sum \left(|\,\rangle\langle\,| + |\,\rangle\langle\,| \right)$$

where the sum runs over all plaquettes including the three possible orientations. The kinetic term controlled by the amplitude t changes the dimer covering of every flippable plaquette, i.e. of every plaquette containing two dimers facing each other, while the potential term controlled by the interaction v describes a repulsion ($v > 0$) or an attraction ($v < 0$) between dimers facing each other. Since a positive v favours configurations without flippable plaquettes, while a negative v favours configurations with the largest possible number of flippable plaquettes, one might expect a phase transition between two phases as a function of v/t. The actual situation is far richer though. As shown by Moessner and Sondhi [14], who calculated the temperature dependence of the structure factor, there are four different phases: (i) A staggered phase for $v/t > 1$, in which the ground-state manifold consists of all non-flippable configurations. (ii) A columnar ordered phase for v/t sufficiently negative. (iii) An ordered phase adjacent to it which probably consists of resonating plaquettes which make a 12-site unit-cell pattern [15]. (iv) A liquid phase with a featureless and temperature independent structure factor. This last phase has been interpreted as a short-range (RVB) phase in which all correlations decay exponentially at zero temperature, an interpretation confirmed by recent Green's function quantum Monte Carlo simulations [16], which have established the presence of topological degeneracy in this parameter range, a clear characteristic of the RVB phase.

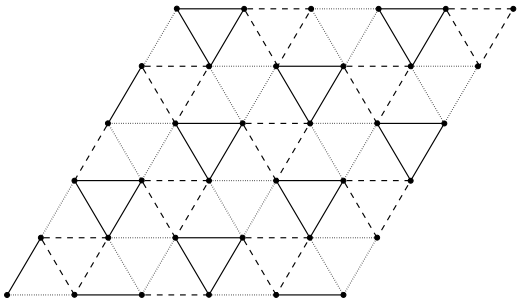

Figure 1. Triangular lattice on which the spin-chirality Hamiltonian is defined. The unitary vector for the bond is indicated by solid lines ($\vec{e}_\mu = \vec{e}_1$), dashed lines ($\vec{e}_\mu = \vec{e}_2$), and dotted lines ($\vec{e}_\mu = \vec{e}_3$).

This result defines a new line of research in the field: indeed, rather than investigating directly the properties of the Heisenberg model on a given lattice, one can try to identify models for which a VB subspace is a reasonable variational subspace, derive an effective QDM, and study it along the same lines as the minimal model on the triangular lattice. In that respect, a natural candidate is the trimerized spin-1/2 Heisenberg model on the kagome lattice. An effective model in terms of the total spin $\vec{\sigma}$ and a chirality pseudo-spin $\vec{\tau}$ per strong triangle has been derived [17, 18]. It is defined on the triangular lattice built by strong triangles and can be written as [19]:

$$\mathcal{H}_0^{\text{eff}} = \frac{J'}{9} \sum_{\langle i,j \rangle} \vec{\sigma}_i \cdot \vec{\sigma}_j (1 - 4\vec{e}_{ij} \cdot \vec{\tau}_i)(1 - 4\vec{e}_{ij} \cdot \vec{\tau}_j), \tag{1}$$

where J' is the weak coupling between the strong triangles of the trimerized lattice, and where the vectors $\vec{e}_{ij}$ have to be chosen among $\vec{e}_1 = (1, 0)$, $\vec{e}_2 = (-\frac{1}{2}, -\frac{\sqrt{3}}{2})$, $\vec{e}_3 = (-\frac{1}{2}, \frac{\sqrt{3}}{2})$ according to the pattern of figure 1. A mean-field decoupling of spin and chirality has identified nearest-neighbour valence bond states as the lowest solutions [18], and, following Rokhsar and Kivelson [13], a QDM has been derived [20]. Unfortunately, it has not yet been possible to study the properties of this model. First of all, they involve kinetic terms on longer loops than the above-mentioned minimal model, but more importantly it is impossible to formulate it in such a way that all off-diagonal matrix elements are negative, so that the quantum Monte Carlo methods that were successful for the minimal model cannot be used.

The effective spin-chirality model has another remarkable feature though: it is formally very similar to the spin–orbital models that are used to describe Mott insulators with orbital degeneracy. Indeed, as discussed in great detail by Kugel and Khomskii [21], when the local symmetry is such that different orbitals can be occupied in the open shell of the magnetic ions of a Mott insulator, this extra degree of freedom can be described by a pseudo spin, and the resulting model is, roughly speaking, of the same form. Given the very different precise forms this model can take for specific systems, a general discussion cannot be attempted here. Rather, we concentrate in the next section on a specific example of a Mott insulator with orbital degeneracy for which we believe that RVB physics might be realized. More general comments will be given in the last two sections of the paper.

2. The spin–orbital model of $LiNiO_2$

The Mott insulator $LiNiO_2$ and its cousin $NaNiO_2$ are isostructural and isoelectronic. The crystal structure can be envisaged as a sequence of slabs of edge sharing octahedra of oxygen

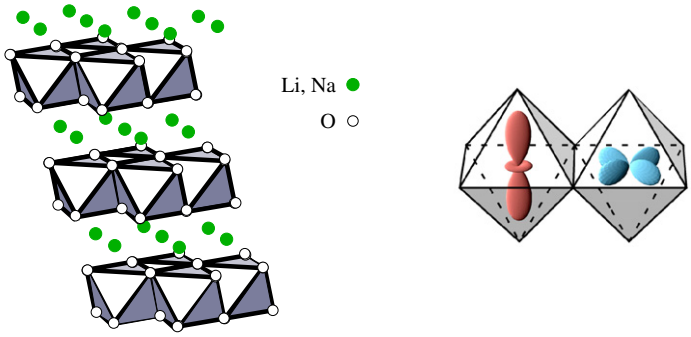

Figure 2. Left: $ANiO_2$ structure. Ni ions are located in the middle of the O octahedra. Right: local structure and degenerate orbitals: $d_{3z^2-r^2}$ (left octahedron) and $d_{x^2-y^2}$ (right octahedron).

O^{2-} ions. Metal ions sit at the centres of the octahedra. There are two kinds of slabs: in A slabs, at the centre of every octahedron there is a Ni^{3+}, whereas in the B slabs, one finds either Li^+ or Na^+ ions. A and B slabs alternate (see figure 2). The Ni ions form well-separated triangular planes. The Ni^{3+} ions are in the $S = 1/2$ low-spin state, which allows for twofold orbital degeneracy between the $d_{3z^2-r^2}$ and $d_{x^2-y^2}$ orbitals (see figure 2).

Surprisingly enough, the two systems have very different properties: $NaNiO_2$ undergoes a high temperature Jahn–Teller distortion, followed at low temperature by the antiferromagnetic ordering of ferromagnetic triangular planes, which makes it a standard example of orbital ordering followed by magnetic ordering [22]. By contrast, no ordering could be detected in $LiNiO_2$, and some kind of freezing seems to take place below 8 K [23]. The best samples of $LiNiO_2$ are non-stoichiometric however: some Li sites are occupied by Ni atoms, and this has been invoked to explain the difference. The trend upon approaching stoichiometry is not clear though, and this striking difference between the two systems, in particular the lack of any sign of a cooperative Jahn–Teller transition in $LiNiO_2$, suggests that we should look for alternative explanations. In the following, starting from a realistic microscopic description of the system, we study the possibility of stabilizing an RVB spin–orbital liquid in the absence of any disorder.

2.1. Microscopic model

A fairly general description of this system is given by a Kugel–Khomskii Hamiltonian defined in terms of Wannier functions centred on the Ni sites by two hopping integrals t_h and t'_h, the on-site Coulomb repulsion U and the Hund coupling J which, on a given bond, takes the form [24]

$$\begin{aligned}\mathcal{H}_{ij} = -\frac{2}{U+J}\Big[&2t_h t'_h \mathbf{T}_i\mathbf{T}_j - 4t_h t'_h T_i^y T_j^y + (t_h - t'_h)^2(\mathbf{n}_{ij}^z\mathbf{T}_i)(\mathbf{n}_{ij}^z\mathbf{T}_j)\\ &+ \tfrac{1}{2}\,(t_h^2 - t_h'^2)\left(\mathbf{n}_{ij}^z\mathbf{T}_i + \mathbf{n}_{ij}^z\mathbf{T}_j\right) + \tfrac{1}{4}(t_h^2 + t_h'^2)\Big]\mathcal{P}_{ij}^{S=0}\\ &- \frac{2}{U-J}\left[4t_h t'_h T_i^y T_j^y + \frac{1}{2}(t_h^2 + t_h'^2) + \frac{1}{2}(t_h^2 - t_h'^2)\left(\mathbf{n}_{ij}^z\mathbf{T}_i + \mathbf{n}_{ij}^z\mathbf{T}_j\right)\right]\mathcal{P}_{ij}^{S=0}\\ &- \frac{2}{U-3J}\left[-2t_h t'_h \mathbf{T}_i\mathbf{T}_j - (t_h - t'_h)^2(\mathbf{n}_{ij}^z\mathbf{T}_i)(\mathbf{n}_{ij}^z\mathbf{T}_j) + \frac{1}{4}(t_h^2 + t_h'^2)\right]\mathcal{P}_{ij}^{S=1} \quad (2)\end{aligned}$$

with the usual definitions for the projectors on the singlet and triplet states of a pair of spins:

$$\mathcal{P}_{ij}^{S=0} = \tfrac{1}{4} - \mathbf{S}_i\mathbf{S}_j \qquad \text{and} \qquad \mathcal{P}_{ij}^{S=1} = \mathbf{S}_i\mathbf{S}_j + \tfrac{3}{4}, \quad (3)$$

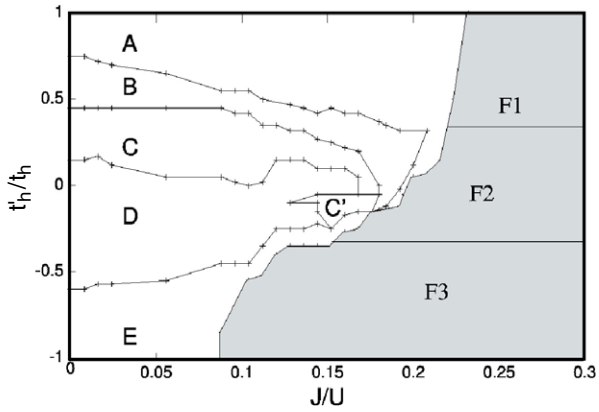

Figure 3. Mean-field phase diagram on a 16-site cluster as a function of hopping integral versus Hund coupling. The grey phase is the ferromagnetic phase, with the classical phase boundaries between different types of orbital ordering.

The vectors $\mathbf{n}^z_{ij}$ depend on the orientation of the bonds and are given by $\mathbf{n}^z_{12} = (0, 0, 1)$, $\mathbf{n}^z_{13} = (\frac{\sqrt{3}}{2}, 0, -\frac{1}{2})$ and $\mathbf{n}^z_{23} = (-\frac{\sqrt{3}}{2}, 0, -\frac{1}{2})$ for the three orientations respectively. The operators $\mathbf{T}_i$ are pseudo-spin operators acting on the orbitals. For the local geometry shown in the right panel of figure 2, t_h and t'_h correspond to the hopping between pairs of $d_{3z^2-r^2}$ and $d_{x^2-y^2}$ respectively, the hopping between the $d_{3z^2-r^2}$ on one site and the $d_{x^2-y^2}$ on the other being zero by symmetry. Of course, all bonds are equivalent, but once a basis, i.e. a pair of local orbitals, has been chosen, the Hamiltonian takes a different form on bonds with different orientations. Note that other forms of the microscopic Hamiltonian including explicitly O orbitals have been used [25–27] with somewhat different conclusions.

2.2. Mean-field phase diagram

Inspired by the results obtained on the trimerized kagome model [18], spin and orbital degrees of freedom can be decoupled in a mean-field way [24]. This leads to a phase diagram in which phases can be distinguished by the mean value of the orbital and/or spin part of the Hamiltonian on each bond. The resulting phase diagram is remarkably rich (see figure 3). Orbital ordering in the ferromagnetic phase has also been discussed in [26].

While the planes of $NaNiO_2$ are known by now to be ferromagnetic, suggesting that $NaNiO_2$ is in one of the ferromagnetic phases, $LiNiO_2$ is expected to be in one of the antiferromagnetic phases. The orbital and spin structure of the antiferromagnetic phases is depicted in figure 4, except for phase A, which consists of $SU(4)$ plaquettes [28] and cannot be described along these lines. Since neither orbital nor magnetic ordering could be detected in $LiNiO_2$, and since phases B and D have a simple orbital ordering pattern while phase E is likely to be antiferromagnetically ordered, let us concentrate on phases C and C′. Both phases are characterized by strong dimer singlets forming different regular dimer coverings of the triangular lattice. On each dimer the orbitals are parallel, and they correspond to $d_{3z^2-r^2}$, $d_{3x^2-r^2}$ or $d_{3y^2-r^2}$ depending on the orientation of the bond. Note that all these orbitals are Jahn–Teller active, leading in all cases to two long and four short Ni–O bonds. One might be tempted to conclude that these phases correspond to two types of valence bond solids with the patterns depicted in figure 4. The mean-field approach has a very remarkable property, however: in addition to the mean-field solutions with lowest energy shown in figure 4, there

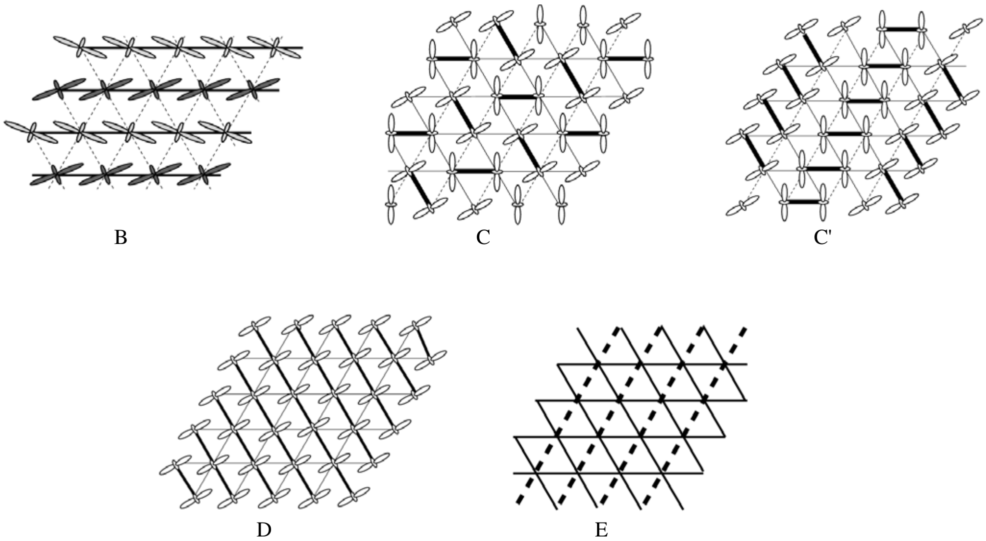

Figure 4. Spin and orbital structure in the singlet phases of the mean-field phase diagram. The solid line indicates AF and the dashed line FM spin correlations.

are several other mean-field solutions of the self-consistent equations with energies very close to the lowest energy corresponding to other dimer coverings of the triangular lattice[5]. In such circumstances, going beyond mean-field is likely to couple these solutions, and the relevant model would then be a QDM describing resonances between these states, a point of view favoured by exact diagonalizations of finite clusters. So it is more appropriate to think of these phases as a region of parameters where all dimer coverings are relevant states for low-energy physics.

2.3. Effective quantum dimer model

Starting from all dimer configurations mentioned in the previous section, a QDM has been derived [30]. It involves competition between kinetic processes and dimer–dimer repulsion. A minimal version of the model is defined by:

$$H = -t \sum \left(|\,/\,/\,\rangle\langle\,\_\,\overline{}\,| + \text{h.c.}\right) - t' \sum \left(\Big|\,{}_{/}\,\overset{\diagdown}{\_}\,\Big\rangle\Big\langle\,\overset{/}{\_}\,{}_{\diagdown}\,\Big| + \text{h.c.}\right)$$
$$+ V \sum \left(|\,/\,/\,\rangle\langle\,/\,/\,| + |\,\_\,\overline{}\,\rangle\langle\,\_\,\overline{}\,| \right), \quad (4)$$

where the sums run over the four-site and six-site loops with all possible orientations. Although the repulsion is a higher order process, and hence quite small, and although the ratio t'/t is in principle fixed by the perturbative expansion, these parameters are treated as free to make contact with the Rokhsar–Kivelson model on the triangular lattice. The main difference with the effective model derived for the trimerized kagome antiferromagnet is that the off-diagonal elements are now all *negative*. This is extremely important in practice since it allows one to use quantum Monte Carlo simulations.

The phase diagram of the model has been derived using exact diagonalizations of finite clusters and Green's function quantum Monte Carlo [30]. As shown before, the most

[5] Such a feature has also been reported in the context of a spin–orbital model of $BaVS_3$ by Mihály *et al* [29].

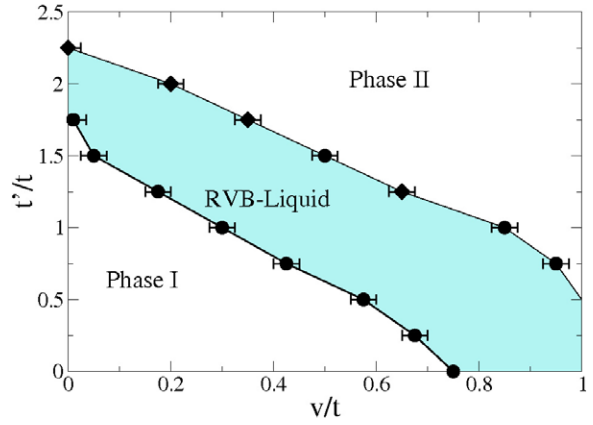

Figure 5. Phase diagram in the $t'-V$ plane. A wide disordered region extends all the way from the standard QDM ($t'/t = 0$ axis) to the purely kinetic QDM ($V/t = 0$ axis). The description of the symbols is given in the text.

convenient way to identify an RVB phase is to look for topological degeneracy since it is at least partially lifted in all other phases. The resulting phase diagram is shown in figure 5. It contains a large RVB liquid phase which connects the relevant parameter range for $LiNiO_2$ ($t'/t \simeq 2$ and V small) to the RVB liquid phase of the minimal model ($t' = 0$). Translated into spin–orbital language, this RVB phase corresponds to a spin–orbital liquid with no symmetry breaking and no phase transition, in agreement with the phenomenology of $LiNiO_2$.

3. Discussion

Let us now comment on how generic the mechanism proposed in the context of the spin–orbital model of $LiNiO_2$ might be. The main ingredients to get an RVB spin–orbital liquid are: (1) the spontaneous formation of dimers; (2) the degeneracy or quasi-degeneracy of the energies of the wavefunctions constructed out of different dimer coverings; (3) the presence of an RVB phase in the relevant QDM. Let us comment on these points separately.

The tendency of spin–orbital models to spontaneously form dimers is well documented. The possibility of stabilizing dimerized ground states due to orbital degeneracy was first put forward by Feiner *et al* in the context of a realistic 3D model [31]. Shortly after, the presence of a dimerized ground state was explicitly proven for a simple minimal 1D model by Kolezhuk and Mikeska [32], a result generalized shortly after by Pati *et al* [33] in the context of a model defined by the Hamiltonian

$$H = \sum_{\langle i,j\rangle} \left[J_1 \vec{S}_i \cdot \vec{S}_j + J_2 \vec{T}_i \cdot \vec{T}_j + K(\vec{S}_i \cdot \vec{S}_j)(\vec{T}_i \cdot \vec{T}_j) \right] \tag{5}$$

with $K > 0$. When $J_1/K = J_2/K = 3/4$, it can be rewritten as

$$H = K \sum_{\langle i,j\rangle} (\vec{S}_i \cdot \vec{S}_j + 3/4)(\vec{T}_i \cdot \vec{T}_j + 3/4). \tag{6}$$

Each term is obviously positive, and since $\vec{S}_i \cdot \vec{S}_j + 3/4$ (resp. $\vec{T}_i \cdot \vec{T}_j + 3/4$) is the projector on the spin (resp. orbital) triplet, the two wavefunctions with alternating spin and orbital singlets are zero energy eigenstates, hence ground states [32]. Pati *et al* have shown that this dimerized phase extends to a very large portion of the phase diagram around this point. From that point

of view, the identification of dimer phases in the context of spin–orbital models of $BaVS_3$ [29] (see footnote 5) and of $LiNiO_2$ [24] is not unexpected, and the tendency to dimerize can be considered to be a generic trend of spin–orbital models.

What seems to be more specific to these spin–orbital models of $LiNiO_2$ and $BaVS_3$ is the quasi-degeneracy of all nearest-neighbour dimer coverings. But in fact, this can be traced back to a rather generic feature of spin–orbital models, namely the remarkable symmetry properties of the orbital part of the Hamiltonian. As can be clearly seen in the spin–orbital model of $LiNiO_2$, the orbital part does not have the same form in the three directions of the triangular lattice, a property encoded in the $\mathbf{n}_{ij}^{z}$ vectors. So the Hamiltonian is only invariant if one simultaneously performs the same rotation in real space and in pseudo-spin space. For purely orbital models, this is known to have remarkable consequences [34–37]. For spin–orbital models, this implies that dimers with different orientations involve different orbital wavefunctions, as can be clearly seen in phases C and C′. What controls the energy of a given dimer configuration is then the residual dimer–dimer interaction. It turns out that simple patterns having all dimers parallel to each other are not naturally favoured if the anisotropy of the orbital part is strong because it is impossible to gain energy in the other directions. On a lattice such as the triangular lattice with a large connectivity, it is then much more favourable to adopt configurations where dimers are not parallel to each other. The energy difference between such configurations, however, is not really significant, and it is better to look at such states as a variational basis.

Finally, too little is known at this stage about RVB phases in QDM to draw general conclusions, but it seems plausible that the presence of an RVB phase between two valence-bond phases is the generic alternative to a first order transition.

To summarize, the tendency toward dimerization is a rather general feature of spin–orbital models. When confronted with a lattice such as the triangular lattice, for which QDMs are known by now to possess RVB phases, there is a real chance for quantum fluctuations to stabilize an RVB ground state.

4. Conclusion

We have shown that orbital degeneracy can, under special but neither unrealistic nor fine-tuned conditions, lead to a spin–orbital RVB ground state. Clearly, this is not the most common situation. Indeed, orbital degeneracy usually leads to a cooperative Jahn–Teller transition, resulting in an effective spin Hamiltonian with a symmetry different from that of the original lattice [21]. This is not the only route to spin–orbital liquid behaviour [38]. However, the tendency of spin–orbital models to spontaneously dimerize is strong enough to make this a promising route to RVB physics. Interestingly enough, a similar conclusion has recently been reached by Baskaran in the context of manganites [39]. Whether $LiNiO_2$ is the first example remains to be seen. To make progress on this issue will require not only further theoretical work to better understand the relevant microscopic model and its possible connection to a QDM, but also, and maybe more importantly, further experimental investigations to unambiguously identify the orbital and magnetic properties of stoichiometric samples.

Acknowledgments

We acknowledge useful discussions with M Ferrero and D Ivanov. This work was supported by the Hungarian OTKA Grant No. T049607 and K6 280, by the Swiss National Fund and by MaNEP.

References

[1] Tsunetsugu H and Arikawa M 2006 *J. Phys. Soc. Japan* **75** 083701
[2] Laeuchli A, Mila F and Penc K 2006 *Phys. Rev. Lett.* **97** 087205
(Laeuchli A, Mila F and Penc K 2006 *Preprint* cond-mat/0605234)
[3] Dagotto E and Rice T M 1996 *Science* **271** 618
[4] Majumdar C K and Ghosh D K 1969 *J. Math. Phys.* **10** 1388
[5] Anderson P W 1973 *Mater. Res. Bull.* **8** 153
[6] Fazekas P and Anderson P W 1974 *Phil. Mag.* **30** 423
[7] Bernu B, Lecheminant P, Lhuillier C and Pierre L 1994 *Phys. Rev.* B **50** 10048
[8] Lecheminant P, Bernu B, Lhuillier C, Pierre L and Sindzingre P 1997 *Phys. Rev.* B **56** 2521
[9] Mambrini M and Mila F 2000 *Eur. Phys. J.* B **17** 651
[10] Syromyatnikov A V and Maleyev S V 2002 *Phys. Rev.* B **66** 132408
[11] Nikolic P and Senthil T 2003 *Phys. Rev.* B **68** 214415
[12] Budnik R and Auerbach A 2004 *Phys. Rev. Lett.* **93** 187205
[13] Rokhsar D S and Kivelson S A 1988 *Phys. Rev. Lett.* **61** 2376
[14] Moessner R and Sondhi S L 2001 *Phys. Rev. Lett.* **86** 1881
[15] Ralko A, Ferrero M, Becca F, Ivanov D and Mila F 2006 *Phys. Rev.* B at press (*Preprint* cond-mat/0607618)
[16] Ralko A, Ferrero M, Becca F, Ivanov D and Mila F 2005 *Phys. Rev.* B **71** 224109
[17] Subrahmanyam V 1995 *Phys. Rev.* B **52** 1133
[18] Mila F 1998 *Phys. Rev. Lett.* **81** 2356
[19] Ferrero M, Becca F and Mila F 2003 *Phys. Rev.* B **68** 214431
[20] Zhitomirsky M E 2005 *Phys. Rev.* B **71** 214413
[21] Kugel K I and Khomskii D I 1982 *Sov. Phys.—Usp.* **25** 232
[22] Lewis M J, Gaulin B D, Filion L, Kallin C, Berlinsky A J, Dabkowska H A, Qiu Y and Copley J R D 2005 *Phys. Rev.* B **72** 014408
[23] Chappel E, Nunez-Regueiro D, Chouteau G, Isnard O and Darié C 2000 *Eur. Phys. J.* B **17** 615
[24] Vernay F, Penc K, Fazekas P and Mila F 2004 *Phys. Rev.* B **70** 014428
[25] Daré A M, Hayn R and Richard J L 2003 *Europhys. Lett.* **61** 803
[26] Mostovoy M V and Khomskii D I 2004 *Phys. Rev. Lett.* **92** 167201
[27] Reitsma A J W, Feiner L F and Oles A M 2005 *New J. Phys.* **7** 121
[28] Penc K, Mambrini M, Fazekas P and Mila F 2003 *Phys. Rev.* B **68** 012408
[29] Mihály G, Kézsmárki I, Zámborszky F, Miljak M, Penc K, Fazekas P, Berger H and Forró L 2000 *Phys. Rev.* B **61** R7831
[30] Vernay F, Ralko A, Becca F and Mila F 2006 *Phys. Rev.* B **74** 054402
[31] Feiner L F, Oles A M and Zaanen J 1997 *Phys. Rev. Lett.* **78** 2799
[32] Kolezhuk A K and Mikeska H J 1998 *Phys. Rev. Lett.* **80** 2709
[33] Pati S K, Singh R R P and Khomskii D I 1998 *Phys. Rev. Lett.* **81** 5406
[34] Nussinov Z, Biskup M, Chayes L and Van Den Brink J 2004 *Europhys. Lett.* **67** 990
[35] Mishra A, Ma M, Zhang F C, Guertler S, Tang L H and Wan S 2004 *Phys. Rev. Lett.* **93** 207201
[36] Douçot B, Feigel'man M V, Ioffe L B and Ioselevitch A S 2005 *Phys. Rev.* B **71** 024505
[37] Dorier J, Becca F and Mila F 2005 *Phys. Rev.* B **72** 024448
[38] Fritsch V, Hemberger J, Büttgen N, Scheidt E W, Krug von Nidda H A, Loidl A and Tsurkan V 2004 *Phys. Rev. Lett.* **92** 116401
[39] Baskaran G 2006 *Preprint* cond-mat/0607369